A Systematic Analysis Of The Error Sources Within The CyberKnife M6 Daily AQA Test

By

Kevin T. Jordan

ESSAY

Submitted to the Graduate School of Wayne State University, Detroit, Michigan in partial fulfillment of the requirements for the degree of

MASTER OF SCIENCE

2015

MAJOR: RADIOLOGICAL PHYSICS

Approved by:

Tewfik Bichay PhD_____

Advisor Date

Jay Burmeister PhD_____

Program Director Date

ACKNOWLEDGEMENTS

I would like to thank Tewfik Bichay PhD, Medical Physics Director, Lacks Cancer Center, Department of Radiation Oncology at Mercy Health St. Mary's Campus located in Grand Rapids, Michigan. Our relationship started with research projects to give me pertinent exposure before entering graduate school and now we have developed this fantastic research project of graduate level material, which has now been accepted to an international conference. This relationship and guidance over the years as been simply invaluable and I will always be grateful for it.

I would also like to thank Alan Mayville MS, Medical Physics Resident, for continued knowledge on the CyberKnife M6 system and brainstorming experimental methods for the success of this project. Finally, Chen Chen MS, Medical Physicist, who I have known since my first research projects and always assisted with any medical physics topics with great enthusiasm. Additionally, I would like to thank the extended staff at Lacks Cancer Center, Department of Radiation Oncology who have always assisted with facilitating medical physics research, without this partnership these projects simply would not exist.

1. TABLE OF CONTENTS

2. LIST OF TABLES

3. LIST OF FIGURES

4. CHAPTERS

4.1. Chapter 1 - Introduction

With the advent of frameless stereotactic radiosurgery (SRS) and stereotactic body radiation therapy (SBRT), the patient now as the freedom of not being restrained in a system such as the CyberKnife M6 system produced by Accuray, compared to that of a framed system such as Gamma Knife. This is a fantastic achievement in patient experience, something the oncology community is constantly striving to provide through continuous improvement. Naturally, a new set of safety precautions and redundancy checks proceeded with the advent of frameless SRS/SBRT. Now that the patient has transformed from a essentially rigid body attached to fixed coordinate system to a free floating body, proper training and the addition of ancillary systems had to be incorporated to essentially ensure a rigid body result in a free floating environment. The greatest tool to assure this has been incorporating image guidance into the radiation therapy treatment room. In combination with the ability to track respiratory motion, patient safety and freedom can simultaneously be provided.

With these imaging and tracking tools of course comes appropriate quality assurance procedures (QA), including a daily automatic quality assurance (AQA), as prescribed by TG-135 [i], test to verify that where the robot thinks it is accurate within <1 mm, as guaranteed by the manufacturer. The objective of this project has been to determine and critically analyze the sources of error within the daily Automatic Quality Assurance (AQA) test used on the CyberKnife M6 system. Like any experiment, system, machinery, computational device there are errors;

systematic and random ones. Just how much error there is versus what is acceptable is what one must concern themselves with.

4.2. Chapter 2 - CyberKnife Robotic Radiosurgery & AQA

With the advent of robotic radiosurgery, of course came additional procedures, specifically quality assurance procedures are what have been the focus of this research project. Figure 4.2.1 below shows a typical treatment room setup for the CyberKnife M6 system, this figure shows the standard treatment couch and not the RoboCouch.

Figure 4.2.1 Typical treatment room setup for CyberKnife M6 Installation

Since one aspect of the project sought to compare fixed collimation cones (fixed circular field size) and the IRIS attachment[ii], Figure 4.2.2 provides a transparent schematic view of this product provided by the manufacturer. It uses a stepper motor, driven by a cam system to mimic a circle by producing a 12-sided polygon.

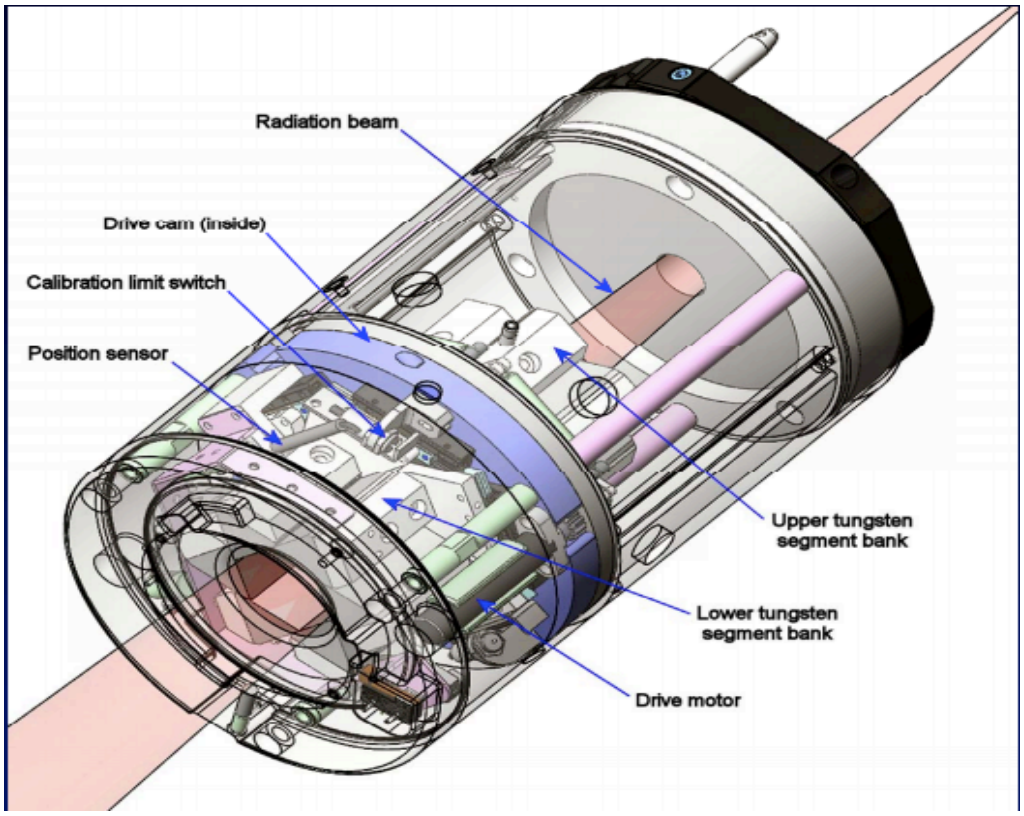

Figure 4.2.2 Close Up Transparent view of IRIS Attachment

The imaging system is of utmost importance in frameless SRS/SBRT treatments, localization accuracy depends on this system and a section view of the setup can be found in Figure 4.2.3 below.

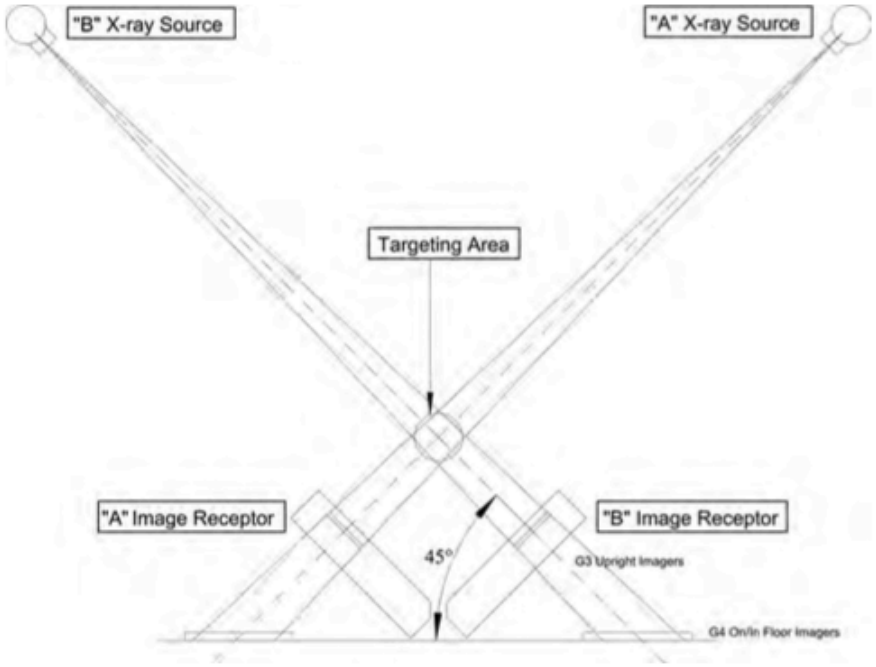

FIG. 2. Image Geometry of image-guidance x-ray system. This view has the observer standing at the head of the couch looking toward the patient.

Figure 4.2.3 Section View of kV Imaging System Setup

The daily AQA process relies upon the use of GAFchromic film, specifically EBT3 or EBT3+. The material makeup and specifications can be found in Figure 4.2.4 below. This film offers fantastic spatial resolution and a wide range of radiation dose usability, from 1cGy to 40Gy.

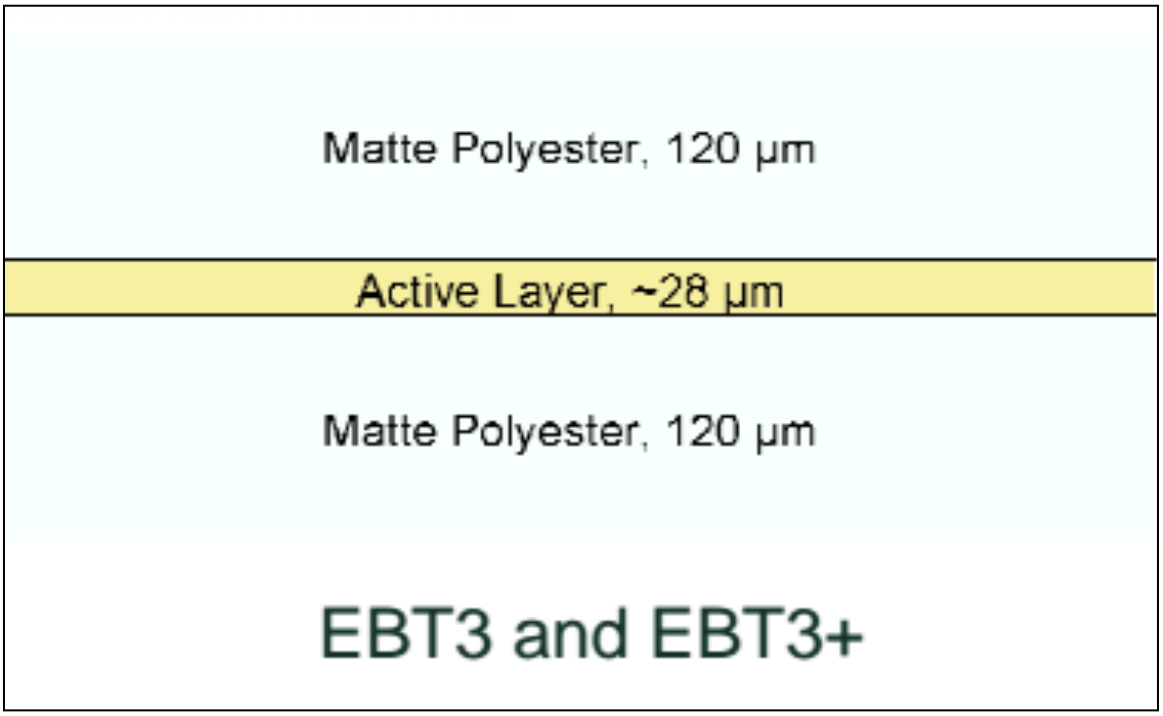

Figure 4.2.4 EBT3 GAFchromic Film Material Makeup

The aforementioned GAFchromic film resides within the dedicated AQA phantom, seen in Figure 4.2.5 below. The AQA test has a dedicated QA plan, generated in the Accuray Multiplan software. Prerequisite to this is of course scanning the AQA phantom in the radiation oncology department's Computed Tomography (CT) simulation scanner. This data is then imported into the Multiplan software and the appropriate AQA plan may be developed and sent to the machine for daily use.

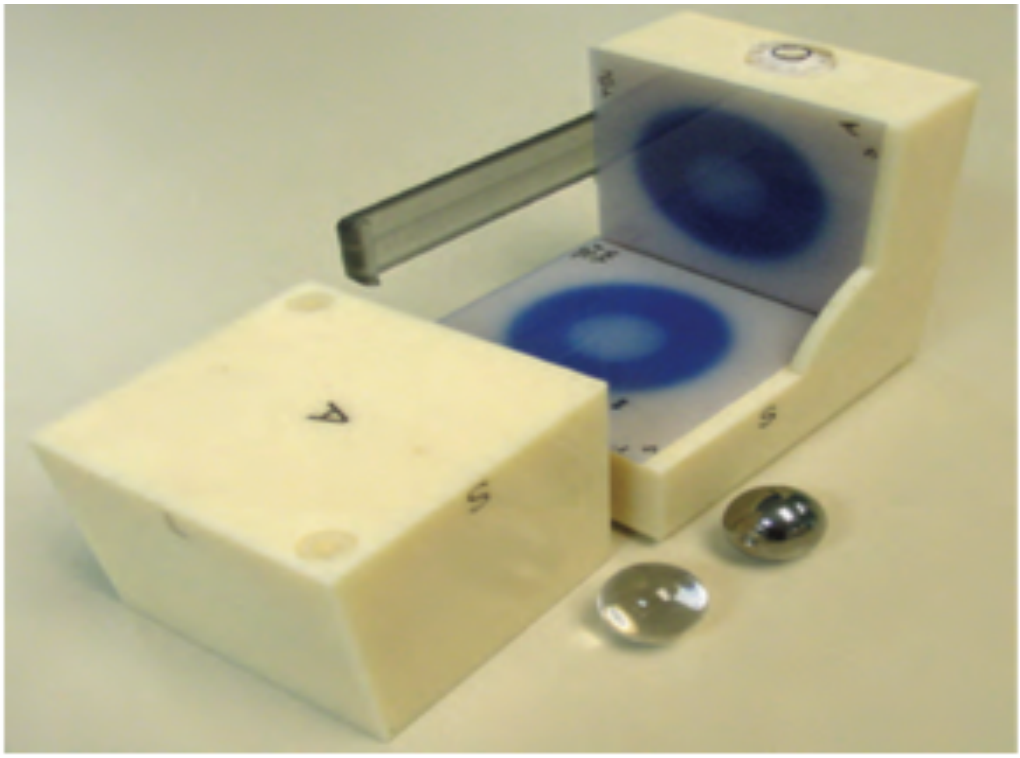

FIG. 8. The AQA phantom showing the orthogonal films after exposure. The clear plastic ball is inserted for the CT scan and replaced by the tungsten ball for the Winston-Lutz test. Figure courtesy of Accuray Inc.

Figure 4.2.5 AQA Phantom Disassembled – Modified Winston Lutz Test

A proprietary algorithm provided by Accuray is then used to analyze beam shadow, eccentricity and pixel intensity based upon the principles and theory of the modified Winston Lutz test[iii], seen in Figure 4.2.6. The algorithm looks at a radial vectors to see the resulting "halo". These results are then equated to patient plane coordinates in order to provide offsets in superior-inferior, right-left, and posterior-anterior planes; thus providing a overall radial (3D) error scalar value.

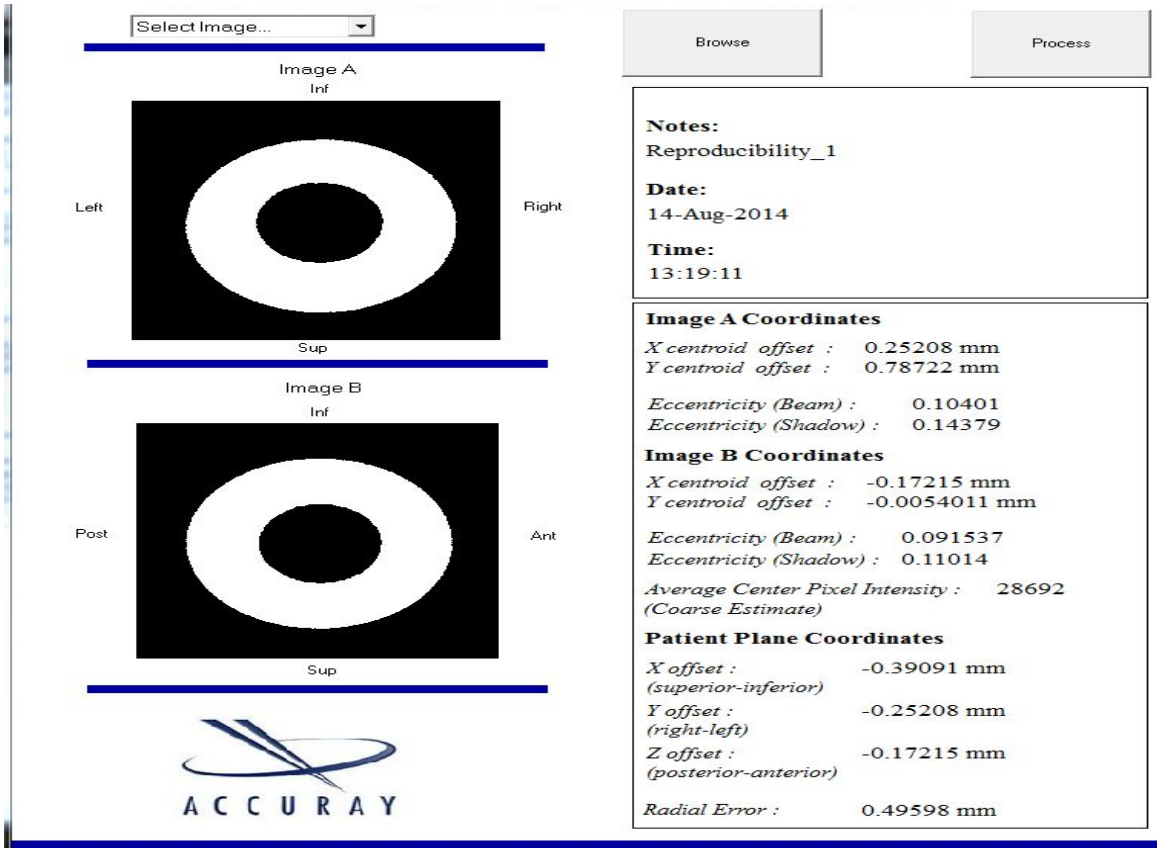

Figure 4.2.6 Accuray AQA Algorithm Results Example – Radial Error

The anthropomorphic skull phantom, Figure 4.2.7, provided useful and efficient date comparisons for kV imaging tracking algorithms such as 6D skull, Fiducial, and Xsight spine, all without ever having to break experimental setup and thus very practical for holding experimental variables constant.

Figure 4.2.7 Skull Phantom

Though not explicitly needed for this research project, the synchrony QA device, Figure 4.2.8, is an important one to mention given its critical use for optical tracking of thoracic movement during treatments. It is also considered another tracking algorithm, though it uses both the kV imaging system and an optical system attached to the patient via a retaining vest.

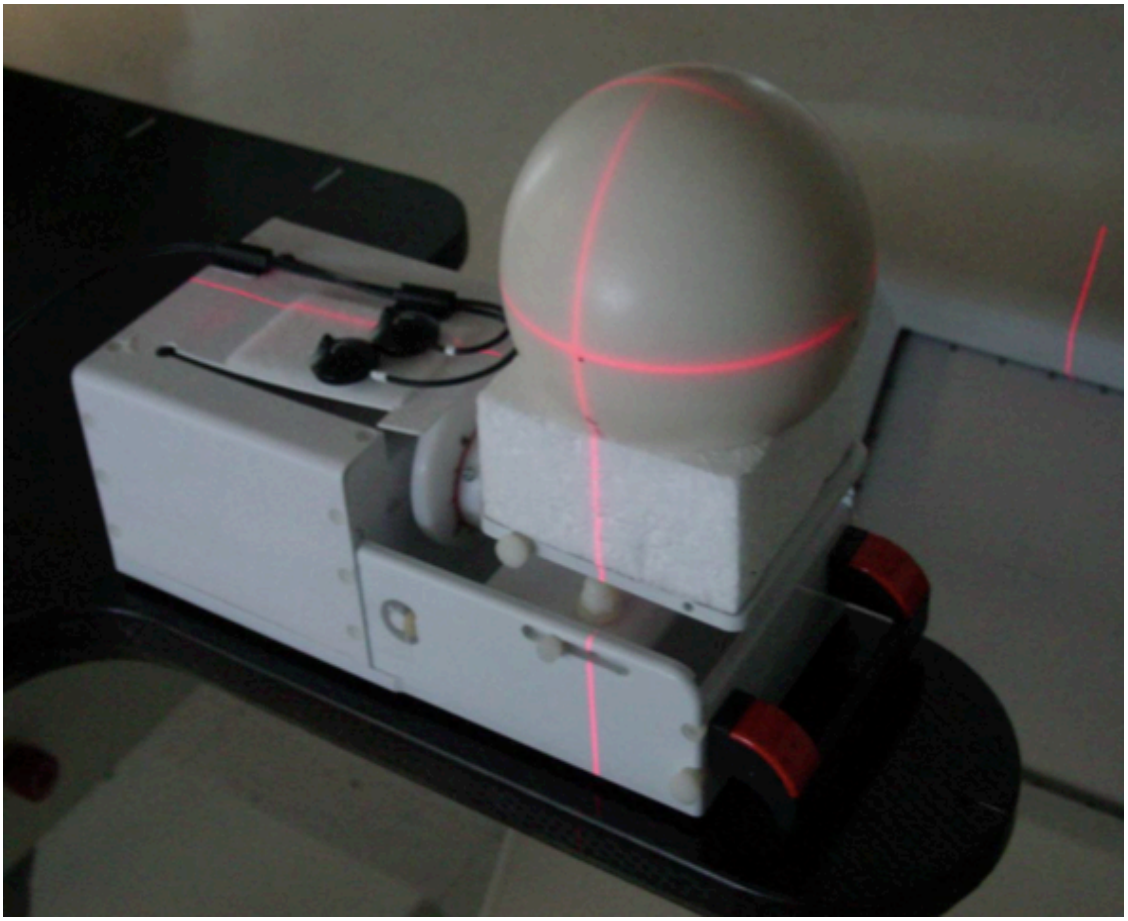

Figure 4.2.8 Synchrony QA Device

A disassembled view of the E2E Ballcube phantom, Figure 4.2.9, again shows orthogonal films used for quantifying total system accuracy; from treatment planning all the way to treatment. This test gives the clinician and physicist a overall system accuracy and confidence in the various components that may be sources of error or inaccuracy in order to track system accuracy over time.

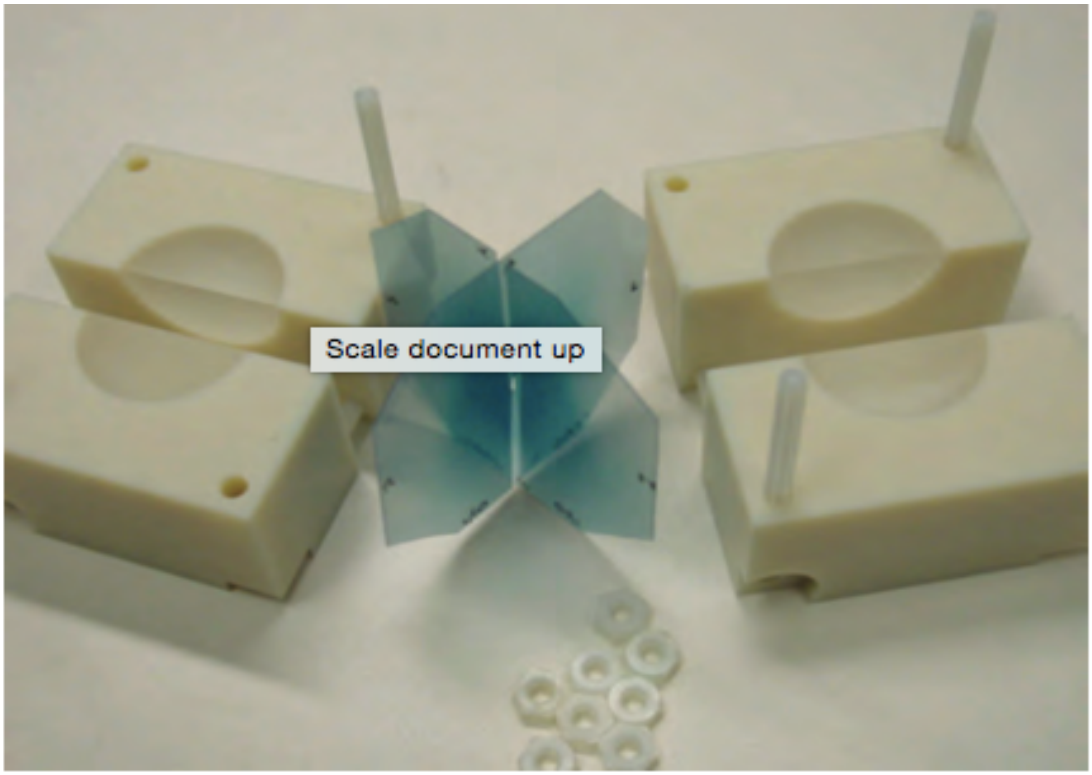

FIG. 9. The E2E ballcube used for fiducial and cranial tracking tests. A hidden target is irradiated. The orthogonal films are analyzed for spatial accuracy of dose delivery and can also be used for film dosimetry as plan verification. Figure courtesy of Accuray Inc.

Figure 4.2.9 E2E Ballcube Disassembled

The results of the E2E test may be witnessed in Figure 4.2.10, providing a total targeting error for the system. TG-135 prescribes this test be done at least once a month.

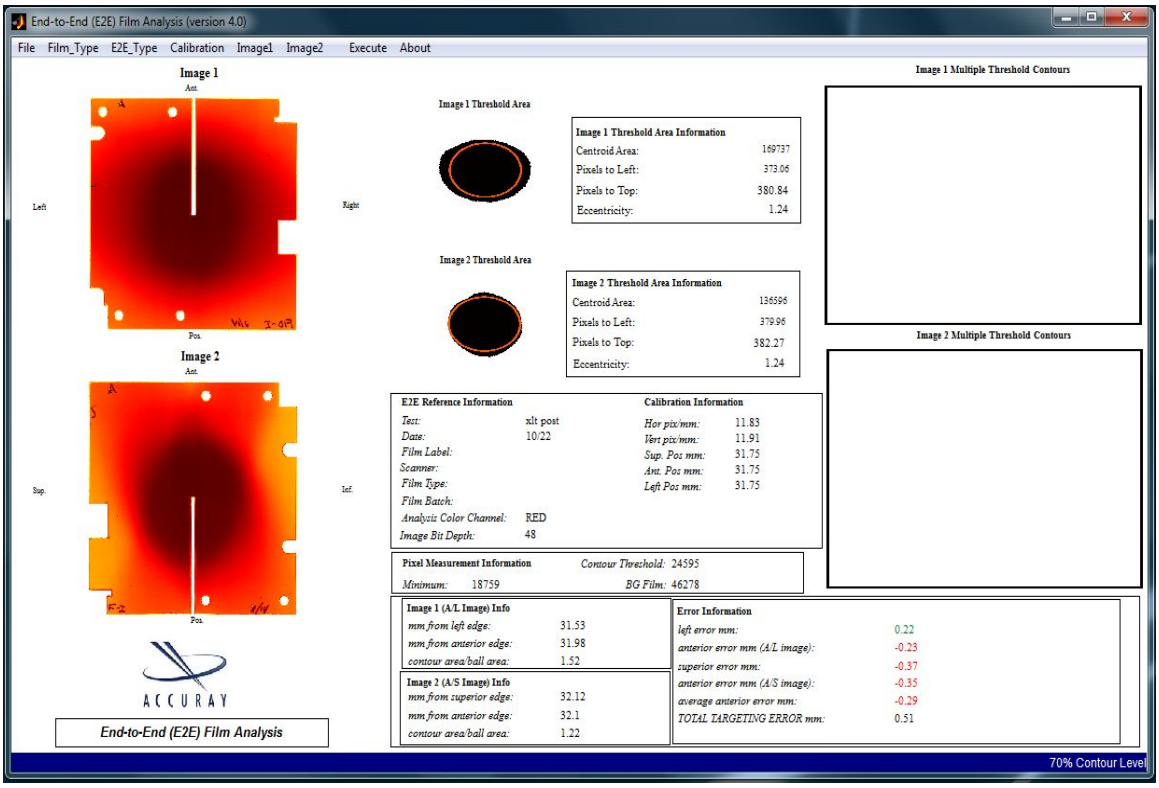

Figure 4.2.10 Accuray E2E Algorithm Results Example – Total Targeting Error

The following three figures, Figure 4.2.11, Figure 4.2.12, and Figure 4.2.13, can be found to itemize the daily, monthly and annual tasks respectively within TG-135. Thus providing safety, quality, and accuracy on system and component level.

IV.B. Daily QA

Section	Item	Tolerance
II.A.2	Safety interlocks (Door, console EMO, Key)	Functional
	CCTV cameras and monitors	Functional
	Audio monitor	Functional
	Collimator assembly collision detector	Functional
II.B.1	Accelerator warm-up: 6000 MU for open chambers, 3000 MU for sealed chambers	N/A
	Accelerator output	<2%: no change needed >2%: adjust calibration
	Detection of incorrect and missing secondary collimator	Functional
III.B.2	Visual check of beam laser and a standard floor mark.	<1 mm
III.C.1	AQA test	< 1 mm from baseline

Figure 4.2.11 TG-135 Daily QA

IV.C. Monthly QA

Section	Item	Tolerance
II.A.2	Safety interlocks.	Functional
II.B.2	Energy constancy.	2%
	Beam symmetry.	>3%
	Beam shape.	>2% Compared to beam data
	Output.	> 2%
II.C.1	Imager alignment.	1 mm or center pixel ± 2 pixels
II.C.3	Contrast, noise, and spatial resolution of amorphous silicon detector.	To be decided by user based on available literature
	Homogeneity/bad pixels.	
II.D	Custom CT model: CT QA (spatial accuracy, electron density).	See TG 66 (Ref. 29)
III.B.1	Verify relative location of beam laser vs. radiation CAX has not changed.	0.5 mm
III.B.2	Visually check isocentric plan to verify beam laser illuminates isocrystal; rotate through path sets each month	Laser on isocrystal for each node
III.C.2	Intracranial and extracranial E2E; set schedule to cycle through each clinically used tracking method and path.	<0.95 mm or <1.5 mm for motion tracking
III.C.3	Nonisocentric patient QA or DQA; ideally performed quarterly.	DTA 2 mm/2%; Synchrony DTA 3%/3 mm
III.D	Observe Synchrony treatment or simulation; listen for unusual noise and visually check for vibrations.	No significant change

Figure 4.2.12 TG-135 Monthly QA

IV.D. Annual QA

Section	Item	Tolerance
II.A.2	EPO button	Functional
II.B.3	TG 51 or IAEA TRS-398, including secondary independent check.	Adjust calibration if >1% difference is found
	Beam data checks on at least three collimators, including largest and smallest collimator (TPR or PDD, OCR, output factors).	To be decided by user
	Dose output linearity to lowest MU/beam used.	1%
II.C.2	Imager kVp accuracy, mA station exposure linearity, exposure reproducibility, focal spot size.	See Table 1 for references
II.C.3	Signal to noise ratio, contrast-to-noise ratio, relative modulation transfer function, imager sensitivity stability, bad pixel count and pattern, uniformity corrected images, detector centering, and imager gain statistics.	Compare to baseline
II.D	TG 53 as applicable.	TG 53 (Ref. 26)
	CT QA (in addition to monthly).	See TG 66 (Ref. 29)
	Data security and verification.	Functional
III.B.2	2nd Order Path Calibration; currently only possible with the help of a service engineer.	Each node < 0.5 mm RMS < 0.3 mm
III.D	Check noise level of optical markers.	<0.2 mm
IV.C	Run Synchrony E2E test with at least 20 deg phase shift; analyze penumbra spread.	To be decided by user
IV.C	Monthly QA.	In addition to tolerances listed above, update all parameters and checklists
IV.B	Daily QA.	Update parameters

Figure 4.2.13 TG-135 Annual QA

4.3. Chapter 3 - Methods & Materials

A systematic analysis of the inherent uncertainties involved in the CyberKnife M6 AQA test was conducted to quantify the uncertainty in each of the components making up the AQA process.

The identified components included the robot positional uncertainty, film scanning precision, film response and the kV imaging system, charted in Figure 4.3.1. A range of 10-20 repeat measurements were carried out for each of these identified components. A modified Winston-Lutz test with orthogonal images was carried out using GAFchromic EBT3 film. The exposure was by a dedicated AQA plan within Accuray's Multiplan Software. The images were scanned on an Epson 10000XL film scanner. The SRS profiler QA device was used to determine the robot positional accuracy and repeatability.

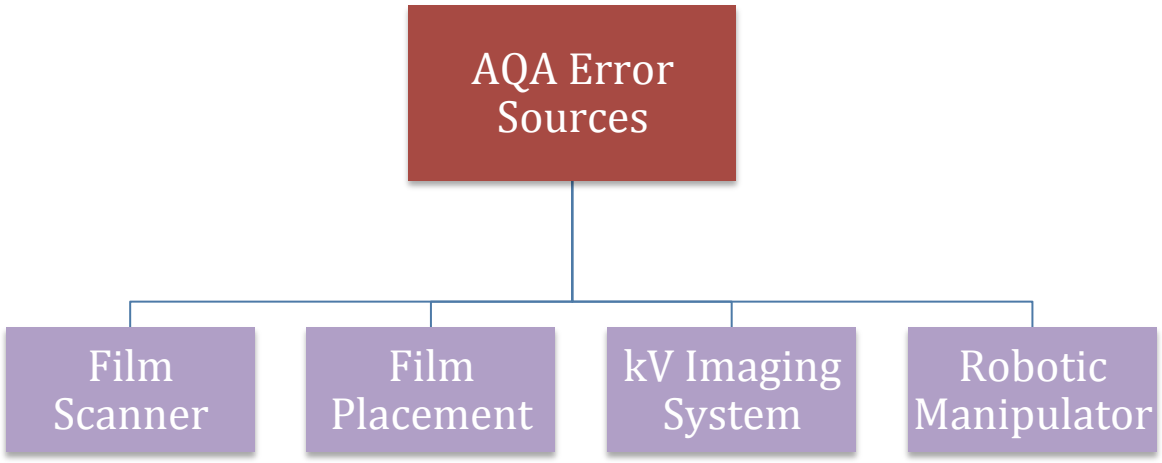

Figure 4.3.1 AQA Error Sources – Break Down Chart

It is helpful to identify the axes of interest when the coarse corrections are provided on the Multiplan software interface, represented in Figure 4.3.2. Recall, the patient data and QA phantom data are imported into the software via the DICOM information within the CT simulation data. The coarse and fine corrections are based upon the Digital Reconstructed Radiograph (DRR) information of that CT simulation data and then compared to that of the live x-ray image taken on the day of treatment or respective QA. The in room lasers can be found for course alignment and then a couch shift (correction) can be done to minimize the CT simulation and live image offsets (deviations). A further read on rigid body transformation algorithms may be of interest for the physicist and interested user[iv].

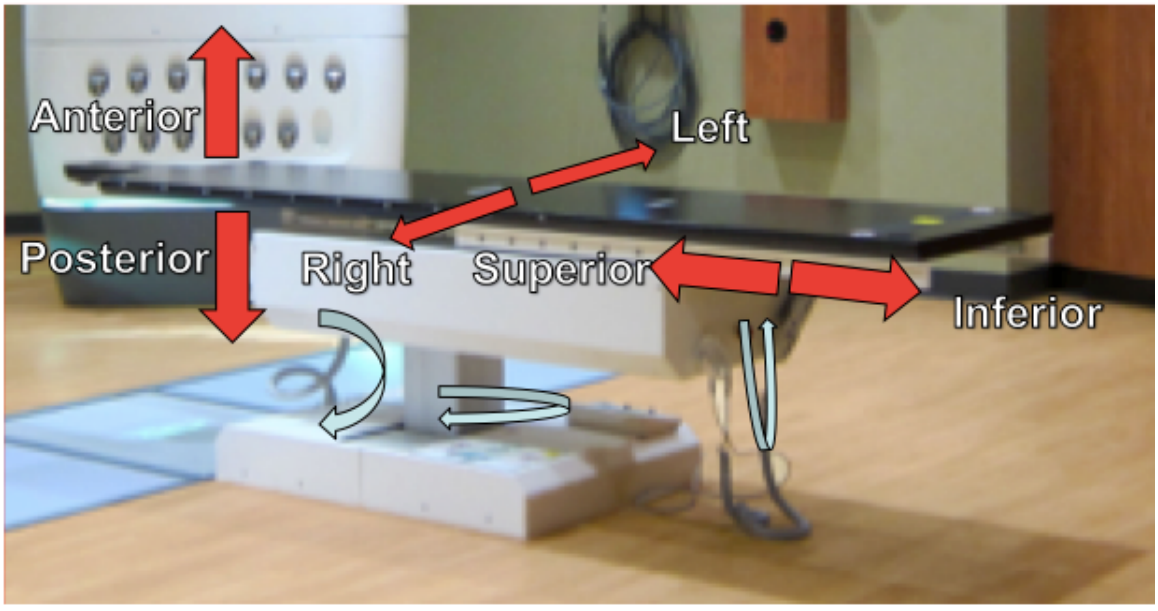

Figure 4.3.2 Corresponding 6axes of Correction from Multiplan

The method and process of daily AQA test can be found outlined in Figure 4.3.3. The AQA phantom has the two EBT GAFchromic films inserted orthogonally, along the Anterior-Superior and Left-Superior planes. The phantom is then placed on the couch, using the acrylic head fixture and in room lasers for course alignment and repeatability.

The Multiplan software can then be used to select the “AQA Plan” and the couch may be corrected to minimal offsets. Leaving twenty minutes after the AQA plan finishes to allow the active layer to finish setting up, one may place the film in the Epson 10000XL scanner. The scanner does not need any color correction features enabled, just simple RGB scanning[v]. The scanned images than may be imported into the Accuray AQA algorithm to process the films and provide the radial error for that AQA test.

Figure 4.3.3 AQA Plan Process

It is helpful to have a close up of the film itself, Figure 4.3.4, and also how it is placed in the scanner. An acrylic fixture is provided for the film to lay one during scanning. Without the fixture, a phenomenon called Newton Rings will occur, a result of two transparent surfaces interacting due to monochromatic light constructive and destructive interference when using EBT2 film [vi]. However EBT3 has overcome this issue by incorporation of a equally thick matte finish layer on each side of the film, as seen in Figure 4.2.4. The use of the acrylic fixture is continued with EBT3 film, but for the sake of repeatability only.

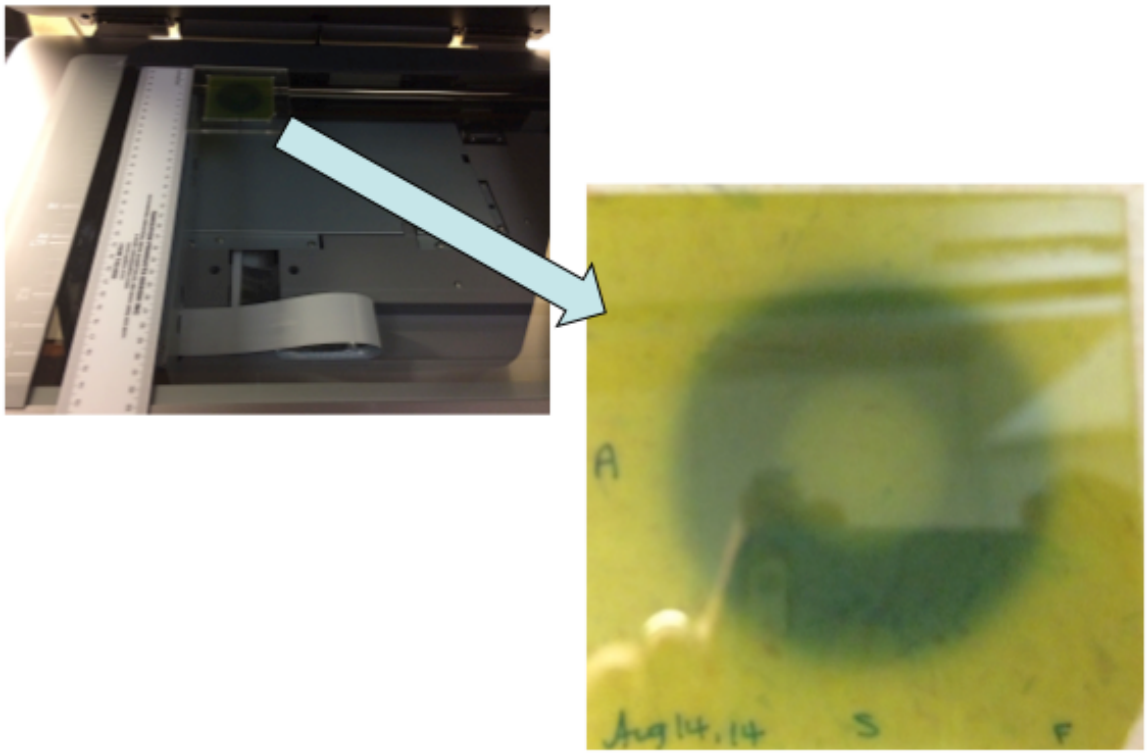

Figure 4.3.4 Scanner & Film Close up

It should be noted the various devices that be used with different tracking algorithms, as witnessed in Figure 4.3.5 below. The AQA phantom on top has Fiducial implanted within the cube, registered during CT simulation and during live QA procedures. The screenshot on the right shows the Fiducial being registered in the Multiplan software; a “drag and drop” method can be use for initial coarse corrections with that of the closest DRR and that of the live image. Green versus white shading is provided to show the differences between the two. The anthropomorphic head phantom can be used for Fiducial, 6D skull and XSight spine tracking algorithms.

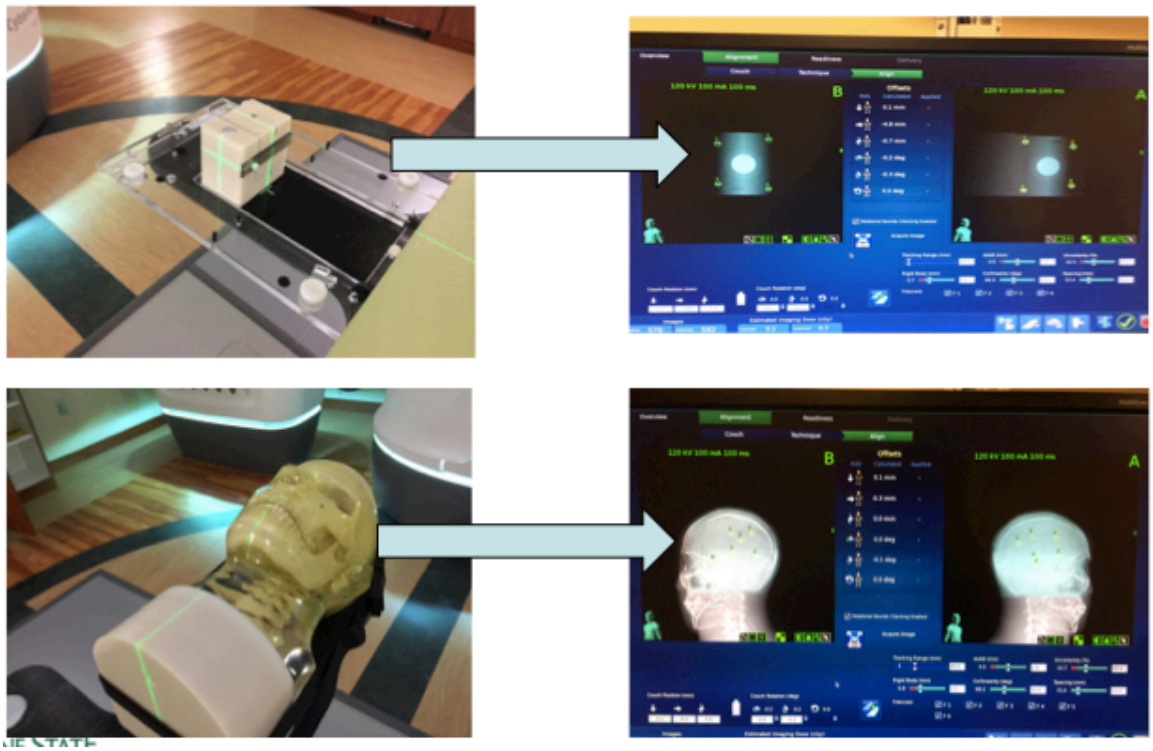

Figure 4.3.5 Fiducial & 6D Skull Algorithm Options

It should be noted that under the hood of CyberKnife is a KUKA industrial robot, a German manufacturer of various robotic suites, as seen in Figure 4.3.6. The difference between that of the typical industrial KUKA robot and the CyberKnife medical KUKA robot is the inclusion of the imaging system for increased localization precision and accuracy and of course the mounting of the physics treatment apparatus on the robotic manipulator, a linear accelerator (LINAC).

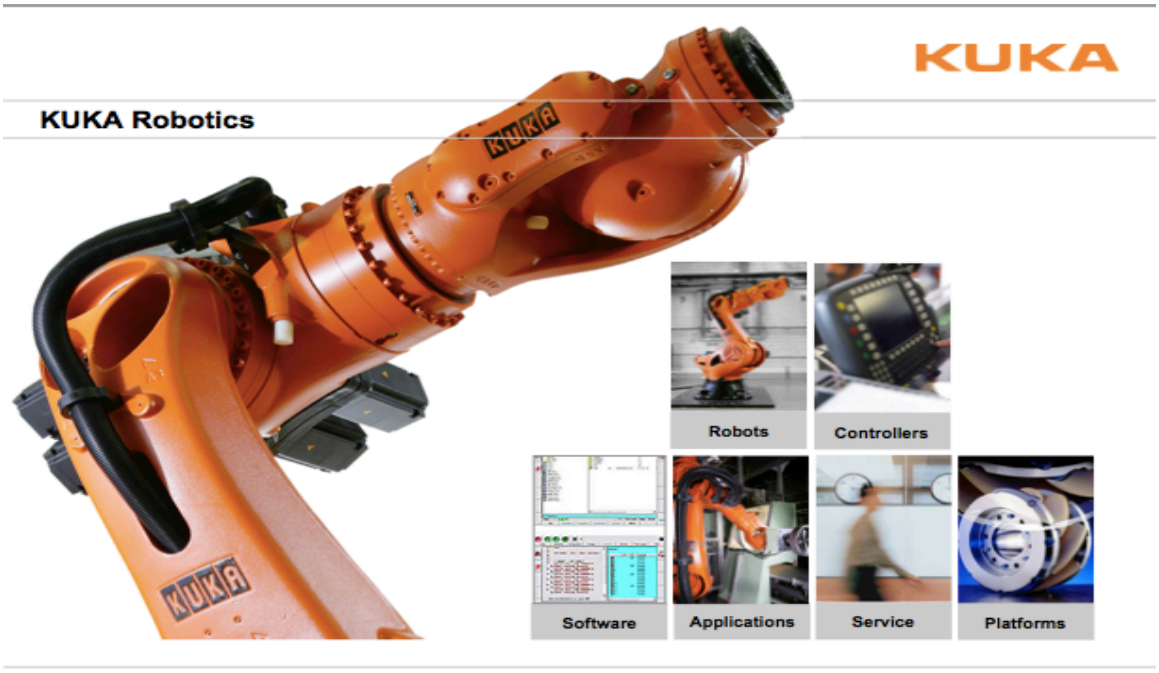

Figure 4.3.6 Under The Hood Robotic Provider – KUKA Robotics

Figure 4.3.7 provides a hardware screenshot, left, and software screenshot, right, of the Sun Nuclear Corp.'s SRS Profiler. Compared to having setup a 3D scanning water tank, this device was preferred for use given its ease of setup provided. First, the precision and accuracy needed to be comfortably quantified before using for data collection. Knowing the diode spacing is manufactured at 4mm[vii], it was hoped that the resolution of the device would be more accurate than this due to the steep dose gradient nature of the CyberKnife treatment delivery. The results were nominal, and will be discussed in the following section.

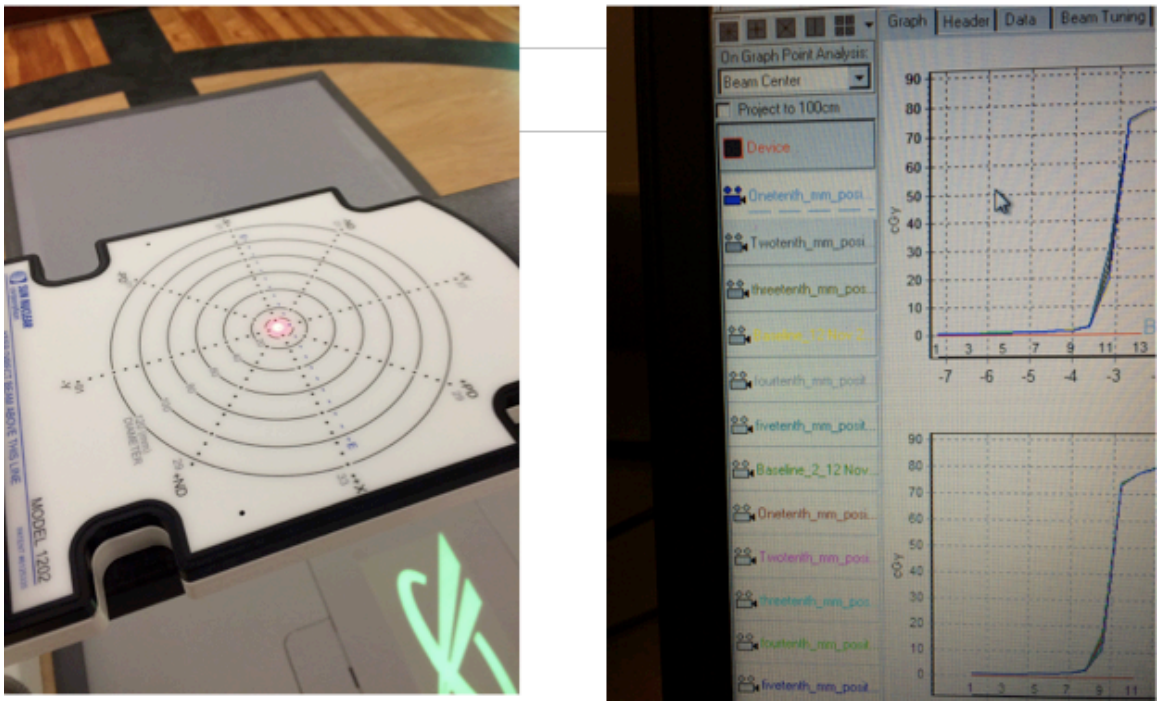

Figure 4.3.7 SRS Profiler Hardware & Software Setups

4.4. Chapter 4 - Results & Discussion

This chapter will be found to highlight the graphical and tabulated data results of the aforementioned four sources of error, and thus four unique experiments conducted to quantify the overall error tolerance of the daily Automatic Quality Assurance test. Equation 4.4-1 below is helpful one to immediately be familiar with, as the radial error is the item at hand that the AQA test comes to be about.

Equation 4.4-1

$$Error_{Radial} = \sqrt{Offset_{Inferior}^{Superior^2} + Offset_{Left}^{Right^2} + Offset_{Posterior}^{Anterior^2}}$$

Visually, Figure 4.4.1 is a useful one to complement that of Equation 4.4-1, as it represents a point in space away from the nominal origin, analogous to the radial error. Recall, the AQA targeting reproducibility test is a film test that checks the robot mastering of the robotic manipulator (treatment delivery) by check checking reproducibility of targeting two beams (vertical & horizontal) by means of a Winston-Lutz test for stereotactic treatment[viii].

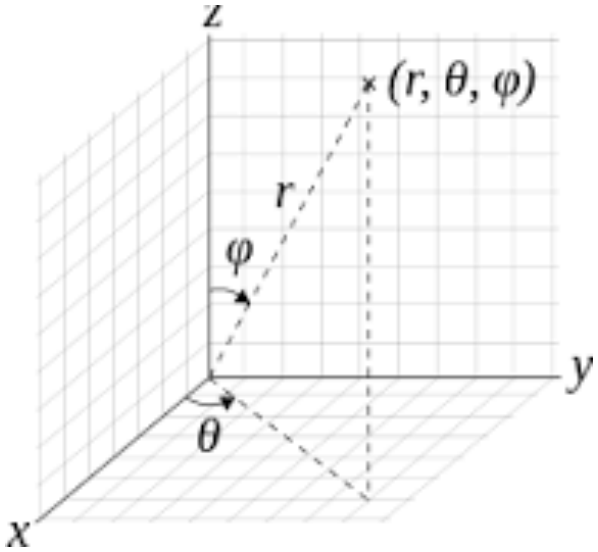

Figure 4.4.1 3D Vector Space – Angular & Translational

Table 4.4.1 can be found to represent the repeat scans of the same film, using IRIS, and never touching that film placement during those repeat scans. A series of ten repeat measurements were taken to get the standard deviation.

Table 4.4.1 Scanner Error - IRIS Patient Plane Values Repeat Film Scans

Patient Plane Coordinates				
X-Offset (superior-inferior)(mm)	Y-Offset (right-left) (mm)	Z-Offset (posterior-anterior)	Radial Error (mm)	
-0.10940	-0.15224	0.11747	0.22124	
-0.11965	-0.15989	0.11778	0.23184	
-0.10901	-0.16041	0.09106	0.21425	
-0.10924	-0.13842	0.09936	0.20240	
-0.11056	-0.16467	0.12803	0.23608	
-0.10889	-0.15039	0.09610	0.20907	
-0.11263	-0.13913	0.13658	0.22516	
-0.09304	-0.16647	0.10186	0.21620	
-0.11132	-0.15355	0.09315	0.21130	
-0.10763	-0.14791	0.10080	0.20851	
-0.10914	-0.15331	0.10822	0.21761	Average (mm)
0.00659	0.00976	0.01569	0.01082	Std. Dev (mm)
0.00208	0.00309	0.00496	0.00342	Std. Dev of Mean

This experiment was repeated on four different days to acquire respective standard deviations to ultimately compile a composite standard deviation of the scanner, as seen in Figure 4.4.2

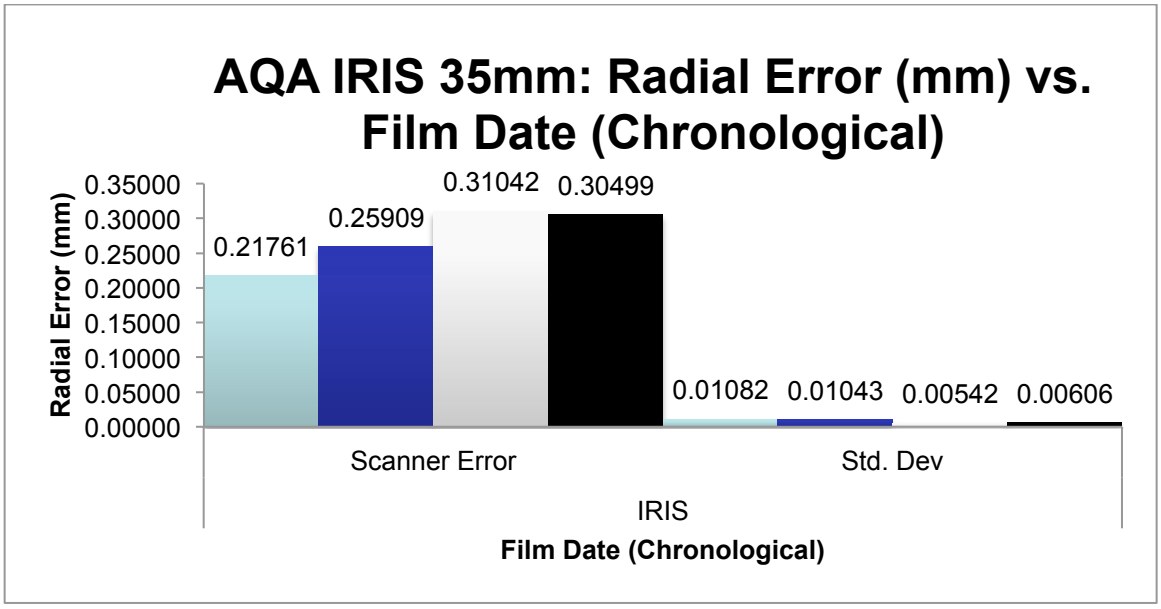

Figure 4.4.2 AQA IRIS Radial Error and Standard Deviation (±1SD)

Again, Table 4.4.2, represent the repeat scans of the same film, but using FIXED cone, and never touching that film placement during those repeat scans. A series of ten repeat measurements were taken to get the standard deviation.

Table 4.4.2 Scanner Error - FIXED Patient Plane Values Repeat Film Scans

Patient Plane Coordinates				
X-Offset (superior-inferior)(mm)	Y-Offset (right-left) (mm)	Z-Offset (posterior-anterior) (mm)	Radial Error (mm)	
-0.11602	-0.15049	0.13626	0.23382	
-0.11093	-0.15049	0.14104	0.23419	
-0.11108	-0.15552	0.13119	0.23181	
-0.11002	-0.16502	0.13533	0.24011	
-0.10852	-0.15220	0.14163	0.23452	
-0.10724	-0.14153	0.08332	0.19614	
-0.09756	-0.15224	0.09402	0.20380	
-0.11548	-0.15637	0.13419	0.23621	
-0.10474	-0.13647	0.13129	0.21641	
-0.10821	-0.16956	0.13776	0.24380	
-0.10898	-0.15299	0.12660	0.22708	Average (mm)
0.00530	0.00975	0.02045	0.01605	Std. Dev (mm)
0.00168	0.00308	0.00647	0.00508	Std. Dev of Mean

This experiment was repeated on three different days to acquire respective standard deviations to ultimately compile a composite standard deviation of the scanner, as shown in Figure 4.4.3.

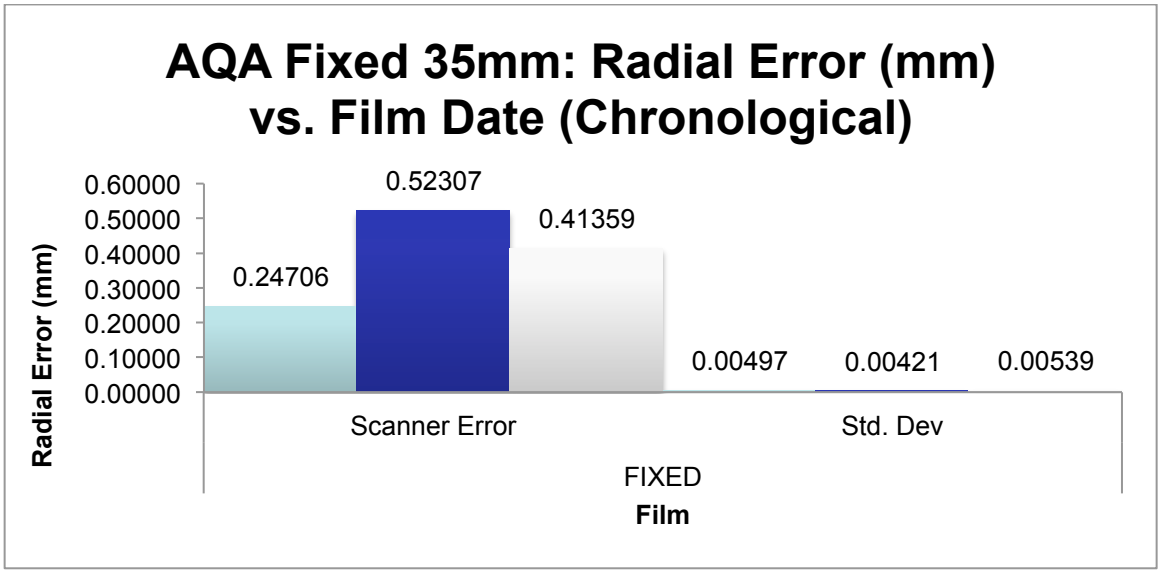

Figure 4.4.3 AQA FIXED Radial Error and Standard Deviation (±1SD)

Figure 4.4.4 and Figure 4.4.5 can be found to represent the repeat scans of the same film, using IRIS and FIXED respectively, and always going through the act of placing that same film on the acrylic fixture before each repeat scan, thus quantifying the error within the placement of the film on the scanner. A series of ten repeat measurements were taken to get the standard deviation. The scanner error must be subtracted out from the final composite standard deviation value.

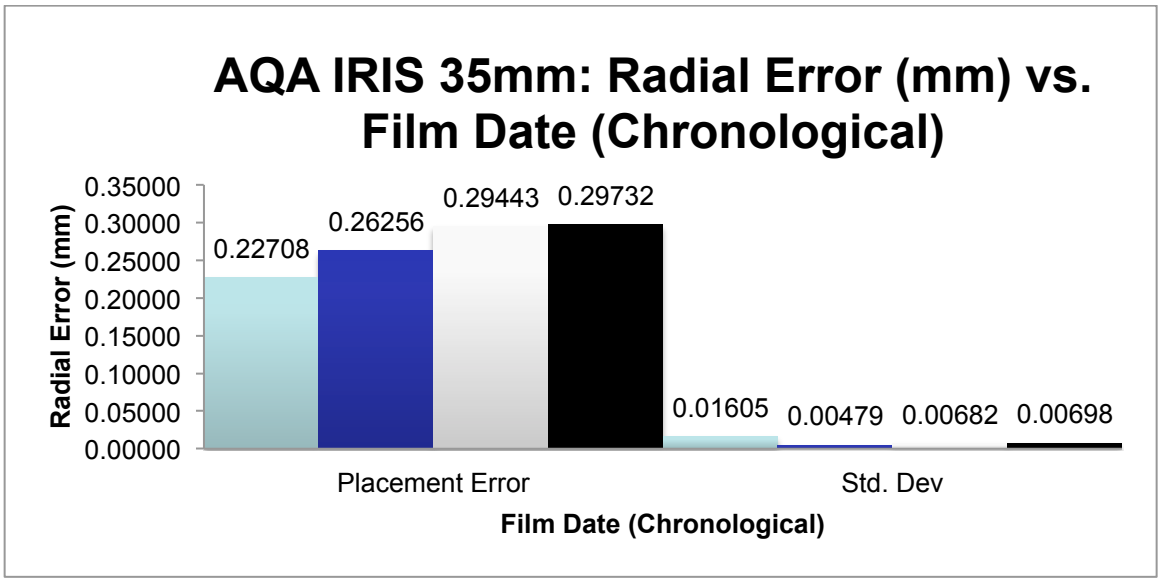

Figure 4.4.4 AQA IRIS Radial Error and Standard Deviation (±1SD)

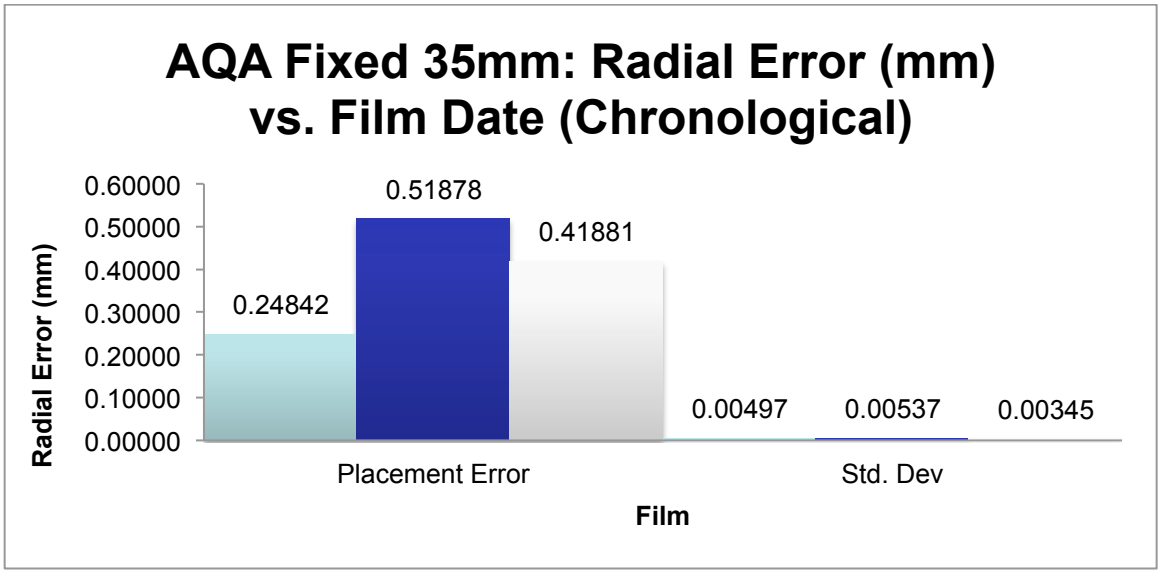

Figure 4.4.5 AQA FIXED Radial Error and Standard Deviation (±1SD)

Figure 4.4.6 and Figure 4.4.7 represent the offsets and standard deviations (error bars) of 6D Skull and Fiducial tracking algorithms respectively. Before coarse corrections are applied, the offsets and deviations were naturally higher, but even with an initial couch correction applied it was evidenced that there are still deviations between x-rays.

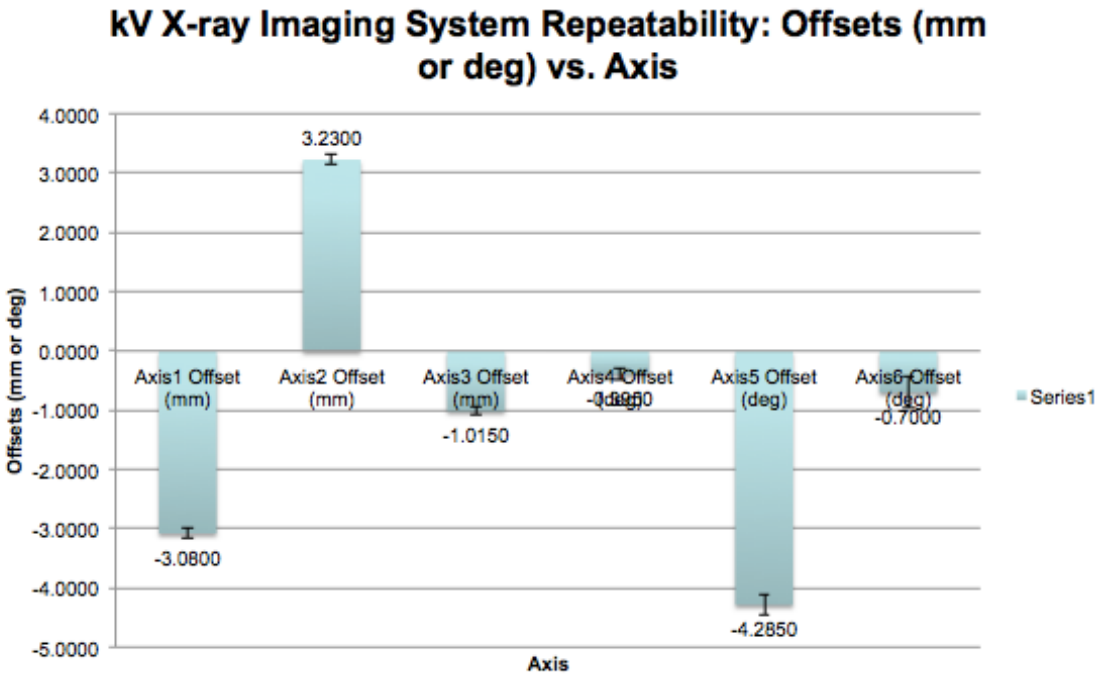

Figure 4.4.6 6D Skull Tracking - Imaging Repeatability

Each set involved a series of 20 x-rays for the given tracking algorithm, and recording the respective translational (three axes) and rotational offsets (three axes) for the six total axes.

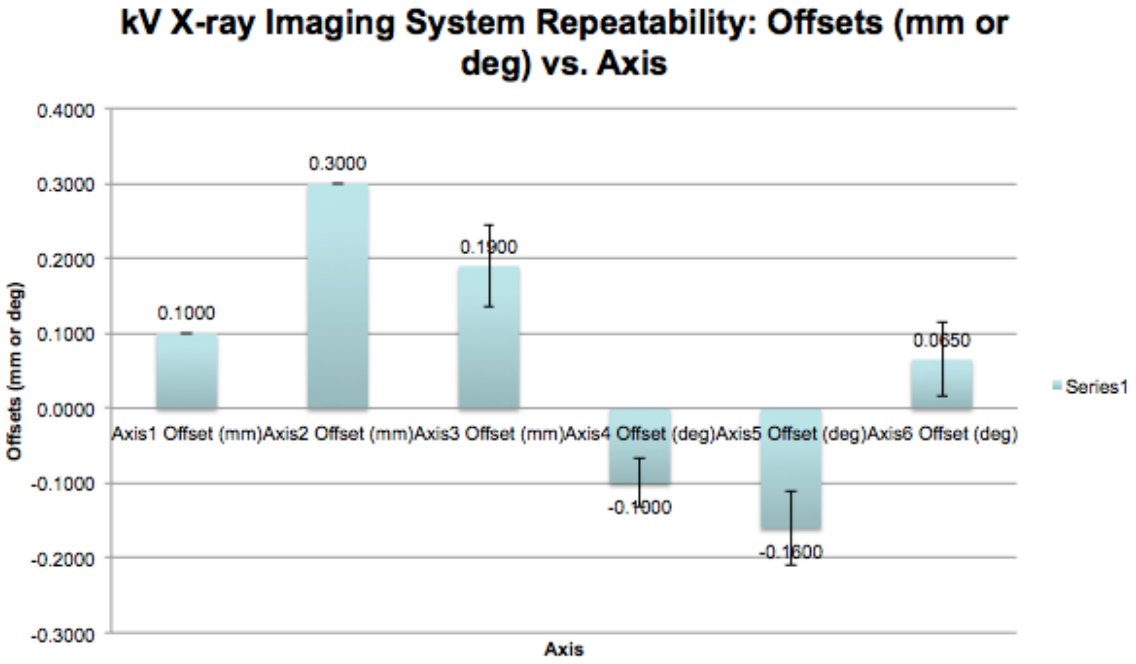

Figure 4.4.7 Fiducial Tracking – Imaging Repeatability

Table 4.4.3 represents the composite deviations of the six different data sets taken for the Fiducial tracking algorithm.

Table 4.4.3 Composite Fiducial Deviations

Tracking Algorithm: Fiducial Deviations						
	Axis1 (mm)	Axis2 (mm)	Axis3 (mm)	Axis4 (deg)	Axis5 (deg)	Axis6 (deg)
1	0.0503	0.0224	0.0999	0.1701	0.0000	0.0224
2	0.0000	0.0000	0.0000	0.0000	0.0503	0.0000
3	0.0000	0.0000	0.0000	0.0000	0.0000	0.0000
4	0.0000	0.0000	0.0452	0.0452	0.0452	0.0452
5	0.0489	0.0000	0.0821	0.0366	0.0470	0.1196
6	0.0000	0.0000	0.0553	0.0324	0.0503	0.0489

Table 4.4.4 represents the composite deviations of the three different data sets taken for the 6D Skull tracking algorithm.

Table 4.4.4 Composite 6D Skull Deviations

Tracking Algorithm: 6D Skull Deviations						
	Axis1 (mm)	Axis2 (mm)	Axis3 (mm)	Axis4 (deg)	Axis5 (deg)	Axis6 (deg)
1	0.0768	0.0923	0.0587	0.0887	0.1755	0.2575
2	0.0000	0.0523	0.0598	0.0366	0.0605	0.0999
3	0.0510	0.0686	0.0510	0.0444	0.0000	0.0000

Table 4.4.5 represents the proof that the SRS profiler is a suitable device for approximately 0.1mm resolution. By programming a world coordinate position using the KUKA pendant based on the center of the SRS profiler and then doing 0.1mm incremental moves, the SRS profiler was able to resolve these fine movements of the robotic manipulator. Thus the 3D water tank was not a necessity to guarantee the accuracy and robustness of the data.

Table 4.4.5 SRS 0.1mm Resolution Proving Grounds

Xrobot = y profiler					
No.	Notes:	nominal Y(cm)	true/raw Y(cm)	Notes:	delta (cm)
0	START	0.02			
1		0.01	0.01	good	0
2		0	0	good	0
3		-0.01	-0.01	good	0
4		-0.02	-0.01	NO	-0.01
5		-0.03	-0.02	residual	-0.01
6		-0.04	-0.03	residual	-0.01
7		-0.05	-0.04	residual	-0.01
8		-0.06	-0.04	NO	-0.02
9		-0.07	-0.05	residual	-0.02
10		-0.08	-0.06	residual	-0.02
		-0.09	-0.07		

Table 4.4.6 shows the repeat SRS profiler measurements while the robotic manipulator was positioned over the center diode. By using the beam center feature in the SRS profiler software, one can normalize, if needed, the X, Y, and diagonal values. This table shows a perfectly stable data set.

Table 4.4.6 SRS Reading Averaging & Stabilization

Baseline Measurement -- SRS Pre-programmed position				
No.	X (cm)	Y (cm)	Positive Diagonal (cm)	Negative Diagonal (cm)
Baseline1	-0.05	0.02	-0.03	-0.05
Baseline2	-0.05	0.02	-0.03	-0.05
Baseline3	-0.05	0.02	-0.03	-0.05
Baseline4	-0.05	0.02	-0.03	-0.05
Baseline5	-0.05	0.02	-0.03	-0.05
Baseline Average	-0.05	0.02	-0.03	-0.05
Baseline Std Dev	0	0	0	0
Baseline Std Error	0	0	0	0

Table 4.4.7 represents the act of moving the robotic manipulator from the perch position to the pre-programmed SRS profiler center position, delivering 100MU (monitor units) and then recording the beam center values accordingly. This data sets a perfect string of ten repeat movements and MU delivery to the center of SRS profiler, however the resolution of the SRS profiler in one plane was proven to be as good as 0.1mm, so that is the resolution of the robotic manipulator.

Table 4.4.7 Robot Localization Repeatability

CyberKnife M6 -- Robot Localization Repeatability				
No.	X (cm)	Y (cm)	Positive Diagonal (cm)	Negative Diagonal (cm)
1	-0.05	0.02	-0.03	-0.05
2	-0.05	0.02	-0.03	-0.05
3	-0.05	0.02	-0.03	-0.05
4	-0.05	0.02	-0.03	-0.05
5	-0.05	0.02	-0.03	-0.05
6	-0.05	0.02	-0.03	-0.05
7	-0.05	0.02	-0.03	-0.05
8	-0.05	0.02	-0.03	-0.05
9	-0.05	0.02	-0.03	-0.05
10	-0.05	0.02	-0.03	-0.05
Average (cm)	-0.05	0.02	-0.03	-0.05
Std. Dev (cm)	0.00	0.00	0.00	0.00
Std. error	0.00	0.00	0.00	0.00

The total film AQA uncertainty using IRIS and FIXED cone was found to be 0.349 and 0.339 millimeters (±3SD) respectively. The Epson 10000XL flatbed scanner was used to scan RGB pixel intensity. The scanner uncertainty was very small; repeat measurements of the same film suggested a scanner precision of 0.015-0.025 millimeters (±3SD). The act of repositioning a film contributed a small uncertainty of 0.0008-0.0014 millimeters (±3SD). The largest uncertainty was due to the imaging system. The kV imaging system fiducial tracking algorithm uncertainty was 0.150 millimeters (±3SD), while the 6D skull algorithm was 0.300 millimeters (±3SD). The SRS Profiler suggested a robot precision uncertainty of 0.1 mm or less along one plane, and thus 0.173 radially (3D).

Table 4.4.8 Composite Maximum Uncertainties (IRIS & FiXED, ± 3SD)

CyberKnife M6 Treatment Delivery Uncertainties - IRIS	
Uncertainty Source	***Uncertainty, mm, +/- 3SD***
Flat Bed Film Scanner	0.025
Film Placement	0.001
kV Imaging System Fiducial Tracking	0.150
Robot Mechanical*	0.173
Total Uncertainty, mm, +/-3SD	***0.349***

CyberKnife M6 Treatment Delivery Uncertainties - FIXED	
Uncertainty Source	***Uncertainty, mm, +/- 3SD***
Flat Bed Film Scanner	0.015
Film Placement	0.001
kV Imaging System Fiducial Tracking	0.150
Robot Mechanical*	0.173
Total Uncertainty, mm, +/-3SD	***0.339***

4.5. Chapter 5 - Conclusions

The total AQA uncertainty appears to be largely due to the kV imaging system. These results suggest an uncertainty of less than 0.1 mm for the film, film scanner, and robot components of the AQA test. The kV imaging system uncertainty could reach 0.3 mm and is the main source of uncertainty.
This information explains greatest weakness in daily CyberKnife QA and may be useful in establishing realistic expectations of daily AQA results.

Table 4.5.1 and Figure 4.5.1 represent the application the minimum and maximum error discussed at the end of Chapter 4 to the four sets of raw radial error taken for IRIS.

Table 4.5.1 IRIS Tolerance Stack Up - Maximum & Minimum Radial Error

IRIS*			
		Tolerance StackUp	
Average (mm)	System Error IRIS, mm, +/- 3SD	-	+
0.2271	0.3493	-0.1222	0.5764
0.2626	0.3493	-0.0867	0.6118
0.2944	0.3493	-0.0548	0.6437
0.2973	0.3493	-0.0519	0.6466

The tabulated and graphical tolerance data shows just how high the true radial error may be for IRIS. For example, a radial error of 0.2271mm ± 0.3493mm = -0.1222mm (minimum radial error) and 0.5764mm (maximum radial error).

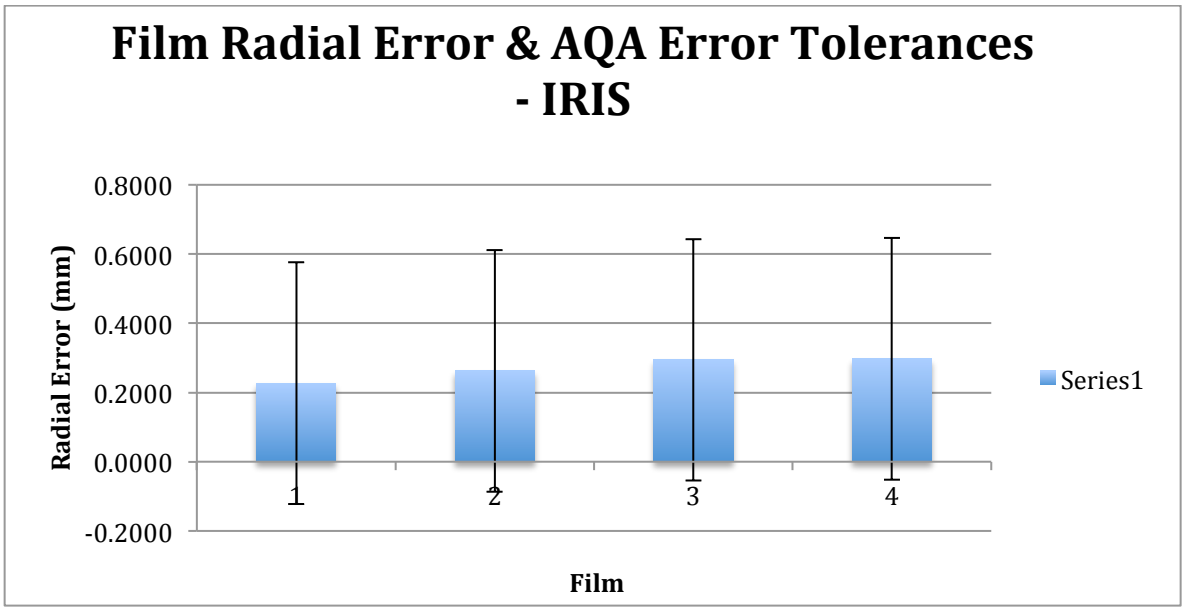

Figure 4.5.1 IRIS Tolerance Stack Up - Maximum & Minimum Radial Error

Table 4.5.2 and Figure 4.5.2 represent the application the minimum and maximum error discussed at the end of Chapter 4 to the three sets of raw radial error taken for FIXED cone.

Table 4.5.2 FIXED Tolerance Stack Up - Maximum & Minimum Radial Error

FIXED*			
		Tolerance StackUp	
Average (mm)	System Error FIXED, mm, +/- 3SD	-	+
0.2484	0.3387	-0.0902	0.5871
0.5188	0.3387	0.1801	0.8574
0.4188	0.3387	0.0802	0.7575

The tabulated and graphical tolerance data shows just how high the true radial error may be for FIXED. For example, a radial error of 0.5188mm ± 0.3387mm = 0.1801mm (minimum radial error) and 0.8574mm (maximum radial error).

Figure 4.5.2 FIXED Tolerance Stack Up - Maximum & Minimum Radial Error

Figure 4.5.3 provides a nice summary of what the clinician should do, if one were to encounter a raw radial error value of the daily AQA test of greater than 0.6 mm. It should also be noted that this value should not be cause for immediate alarm, as the value could be much lower than that raw value for the day. The tolerance has a minimum and maximum and the most important aspect of this project is to understand the potential areas of weakness, and thus the itemized errors and awareness for the realistic expectations of this daily test.

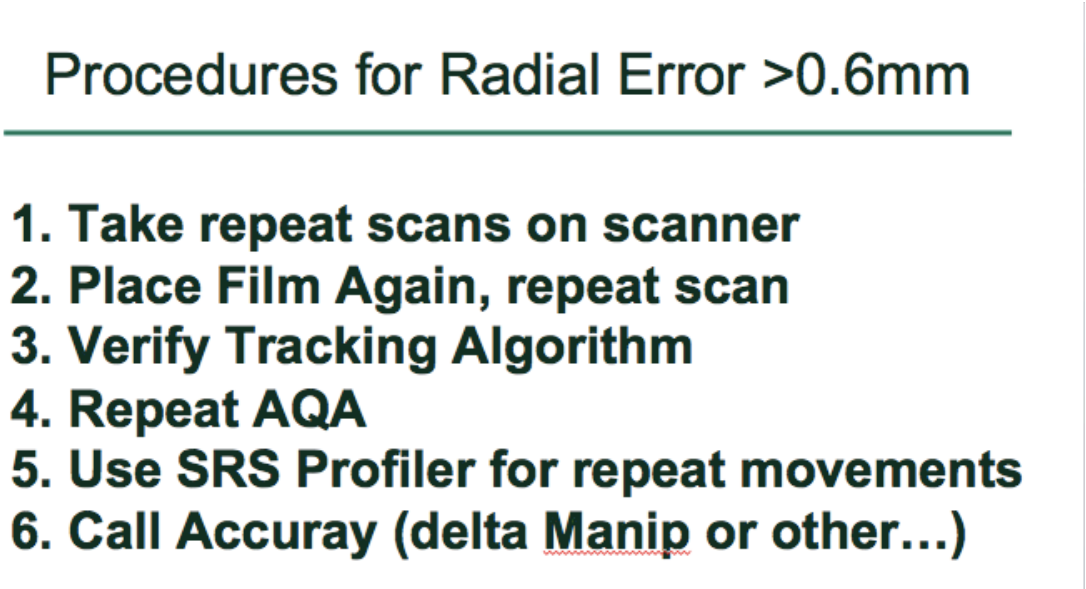

Figure 4.5.3 Procedures for Raw Radial Error >0.6mm

5. ABSTRACT

A SYSTEMATIC ANALYSIS OF THE ERROR SOURCES WITHIN THE CYBERKNIFE M6 DAILY AQA TEST

by

KEVIN TODD JORDAN

JUNE 2015

Advisor: Tewfik Bichay, PhD

Major: Radiological Physics

Degree: Master of Science

Objectives: To determine and critically analyze the sources of error within the daily Automatic Quality Assurance (AQA) test used on the CyberKnife M6 system.

Methods: A systematic analysis of the inherent uncertainties involved in the CyberKnife M6 AQA test was conducted to quantify the uncertainty in each of the components making up the AQA process. The identified components included the robot positional uncertainty, film scanning precision, film response and the kV imaging system. A range of 10-20 repeat measurements were carried out for each of these identified components. A modified Winston-Lutz test with orthogonal images was carried out using GAFchromic EBT3 film. The exposure

was by a dedicated AQA plan within Accuray's Multiplan Software. The images were scanned on an Epson 10000XL film scanner. The SRS profiler QA device was used to determine the robot positional accuracy and repeatability.

Results: The total film AQA uncertainty using IRIS and FIXED cone was found to be 0.349 and 0.339 millimeters (±3SD) respectively. The Epson 10000XL flatbed scanner was used to scan RGB pixel intensity. The scanner uncertainty was very small; repeat measurements of the same film suggested a scanner precision of 0.015-0.025 millimeters (±3SD). The act of repositioning a film contributed a small uncertainty of 0.0008-0.0014 millimeters (±3SD). The largest uncertainty was due to the imaging system. The kV imaging system Fiducial tracking algorithm uncertainty was 0.150 millimeters (±3SD), while the 6D skull algorithm was 0.300 millimeters (±3SD). The SRS Profiler suggested a robot precision uncertainty of 0.1 mm or less.

Conclusion: The total AQA uncertainty appears to be largely due to the kV imaging system. These results suggest an uncertainty of less than 0.1 mm for the film, film scanner, and robot components of the AQA test. The kV imaging system uncertainty could reach 0.3 mm and is the main source of uncertainty. This information explains greatest weakness in daily CyberKnife QA and may be useful in establishing realistic expectations of daily AQA results.

6. REFERENCES

[i] AAPM (2011). Task Group 135: Quality Assurance for Robotic Radiosurgery.

[ii] Accuray Inc. IRIS Variable Aperture Collimator for the CyberKnife Robotic Radiosurgery System: Design, Beam Properties, and Clinical Benefits.

[iii] D. Shepard. Quality Assurance in Stereotactic Radiosurgery and Fractionated Stereotactic Radiotherapy

[iv] D.W. Eggert, A. Lorusso, and R.B. Fisher. Estimating 3-D Rigid body transformations: a comparision of four major algorithms.

[v] J.E. Matney, B.C Parker, D.W Neck, G. Henkelmann, I.I Rosen. Evaluation of a commercial flatbed document scanner and radiographic film scanner for radiochromic EBT film dosimetry. 2010.

[vi] D.F. Lewis. A Guide to Radiochromic Film Dosimetry with EBT2 and EBT3. April 2014.

[vii] SRS Profiler Reference Guide. August 2012.

[viii] Accuray Inc. CyberKnife System: Periodic QA Requirements.